Casimir force between composite materials containing nonspherical particles

J. Sun,[1,2] X. K. Hua,[1] A. V. Goncharenko,[3] and L. Gao[1,*]

[1]*Jiangsu Key Laboratory of Thin Films, Department of Physics, Soochow University, Suzhou 215006, China*

[2]*Department of Mathematics and Physics, Suzhou University of Science and Technology, Suzhou 215009, China*

[3]*Institute of Semiconductor Physics, National Academy of Sciences of Ukraine, Kyiv 03028, Ukraine*

(Received 16 September 2012; published 16 April 2013)

The Casimir force between metal-dielectric composite slabs containing nonspherical particles is investigated. The composite slab may have the symmetric (the nonspherical metal particles and spherical dielectric particles are randomly distributed) or asymmetric microstructure (the nonspherical metal particles are randomly embedded in the dielectric host medium), and the corresponding effective permittivity is described by the generalized Bruggeman effective medium approximation or generalized Maxwell-Garnett approximation. As a consequence, the Casimir force can be controlled by the volume fraction and the particles' shape. It is found that the Casimir force achieves a minimal value for spherical particles, and the magnitude of Casimir force can become strong for nonspherical particles. In addition, the Casimir force for the metal-dielectric composites with the symmetric microstructure shows a fast change at the shape-dependent percolation threshold, above (below) which the composite slab is metallic (dielectric). Our study may be of great interest for making precise comparisons between theoretical and experimental results on the Casimir force.

DOI: 10.1103/PhysRevA.87.042509 PACS number(s): 31.30.jh, 78.20.Ci, 77.84.Lf, 78.67.Bf

I. INTRODUCTION

The Casimir force between two parallel perfect conductor plates was first predicted to validate the existence of zero-point energy in vacuum by Casimir in 1948 [1]. Despite its small magnitude, the force was still observed in recent experiments with high precision [2–7]. The Casimir force (usually attractive) should be considered carefully due to the important role for the applications in microelectromechanical systems and nanoelectromechanical systems, For some reviews, we refer the readers to Refs. [8–11].

It is evident that the Casimir force is largely determined by the material properties such as the permittivity and/or the permeability [12–14]. Since these material properties are controlled by the adjustment of the external magnetic field and temperature, one can realize the field-dependent and temperature-dependent Casimir force [15,16]. Due to recent advances in the development of metamaterials, it is expected that the Casimir force may be significantly influenced. For instance, Yang *et al.* investigated the Casimir force between slabs of left-handed materials and found that the force for left-handed material with sufficiently large bandwidth of negative refraction is generally greater than that for ordinary dielectric [17]. In addition, scientists found that in anisotropic and chiral metamaterials, both attractive and repulsive forces can exist, and the sign of the force depends on the degree of optical anisotropy [18] and the magnitude of the chirality [19].

On the other hand, the Casimir force between inhomogeneous composite materials has also received much attention. By using two-phase aerogels, it was possible to reduce the magnitude of the Casimir force [20]. Actually, aerogels can be regarded as the composite materials in which air bubbles are embedded in the SiO_2 host medium, and the Maxwell-Garnett approximation was adopted to estimate the effective permittivity of the aerogels. Later, physical restrictions on the Casimir interaction of metal-dielectric metamaterials with the aid of effective medium theory were investigated [21]. More recently, several effective medium theories were applied to investigate the effective permittivity of Au/SiO_2 composites, in which the particles are spherical in shape, and then the Casimir force between such composites was calculated using Casimir-Lifshiz theory [22]. It was concluded that the choice of the effective medium theory is critical in making precise comparisons between theory and experiment.

In this paper, we shall investigate the Casimir force between composite systems of nonspherical particles. Our focus is to study the effect of particles' shape, characterized by the depolarization factor, on the Casimir force between composite slabs. The nonspherical shape was found to play an important role for the effective linear and nonlinear dielectric responses [23] and near-field superlens from composites [24,25], bistable Goos-Hanchen shift [26]. Actually, in real experiments, the shape of granular inclusions usually deviates from the spherical one. Here, the composite systems for studying the Casimir force are two-phase metal-dielectric composites in which ellipsoidal metal particles such as Au of volume fraction f and spherical dielectric particles such as SiO_2 of volume fraction $1-f$ are randomly distributed, or in which the ellipsoidal metal particles of volume fraction f are randomly embedded in the dielectric host medium. The composites of the first kind can be called symmetric composites because both metal and dielectric phases may be considered as inclusions embedded in an effective medium, while the composites of the second kind can be called asymmetric, because only one (metal) phase may be considered as inclusions embedded in the dielectric host. Furthermore, we adopt the generalized effective medium approximation (GEMA) [27,28] or generalized Maxwell Garnett approximation (GMGA) [29], respectively, to estimate the effective permittivity by taking into account the shape of metallic particles. With the effective permittivity of composites at hand, one can take one step forward to investigate the Casimir force between such composite slabs. For our systems, both the volume fraction of metallic particles and the particles'

*Corresponding author: leigao@suda.edu.cn

shape can be adjusted simultaneously, resulting in the tunable Casimir force. In addition, within GEMA, we pay attention to the behavior of Casimir force near the percolation threshold of the composite system, in which the metal-insulator transition takes place [30].

The paper is organized as follows. In Sec. II, we first outline the Casimir-Lifshiz theory for the Casimir force between the composite slabs with symmetric or asymmetric microstructure. Both GEMA and GMGA are provided to derive the effective permittivity of composite materials by taking into account the nonspherical shape of metal particles. In Sec. III, numerical results and possible interpretations about the influence of particles' shape and the volume fraction on the Casimir force are given and the percolation effects on the Casimir force are discussed. Our conclusions are presented in Sec. IV.

II. MODEL AND THEORY

Let us consider the Casimir force between two semi-infinite composite slabs separated by a distance d. The slabs are labeled as slab A and B. Each composite slab is assumed to possess the symmetric microstructure where the ellipsoidal metallic particles with permittivity ε_1 and volume fraction f, and spherical dielectric particles with permittivity ε_2 and volume fractions $1-f$, are randomly distributed. To consider the effect of the volume fraction and the particles' shape, the effective permittivity $\varepsilon_e^{A(B)}$ of such composite slab $A(B)$ should be first investigated. For our studied model, the Casimir force per unit area can be written as [17,18,31]

$$F_C = \frac{\hbar}{2\pi^2}\int_0^\infty d\xi \int k\,dk \sqrt{\frac{\xi^2}{c^2}+k^2} \times \sum_{N=\mathrm{TE,TM}} \frac{r_N^A(\xi,k) r_N^B(\xi,k) e^{-2d\sqrt{\frac{\xi^2}{c^2}+k^2}}}{1-r_N^A(\xi,k) r_N^B(\xi,k) e^{-2d\sqrt{\frac{\xi^2}{c^2}+k^2}}}, \quad (1)$$

where k is the transverse wave vector parallel to the slab surface and $r_N^{A(B)}$ is the reflection coefficient of each slab for a given transverse-electric ($N=\mathrm{TE}$) and transverse-magnetic ($N=\mathrm{TM}$) polarized wave. After introducing the imaginary frequency analysis with $\omega = i\xi$ and performing the polar coordinates transformation $\xi/c = \kappa\cos\phi$, $k = \kappa\sin\phi$, and $x = 2\kappa d$ [17], we obtain the normalized force η, which is the ratio of the force to the Casimir force between two perfectly conducting plates F_0 ($=\pi^2\hbar c/240d^4$),

$$\eta = \frac{15}{2\pi^4}\int_0^\infty dx\, x^3 \int_0^{\frac{\pi}{2}} \sin\phi\, d\phi \times \sum_{N=\mathrm{TE,TM}} \frac{r_N^A(x,\phi) r_N^B(x,\phi) e^{-x}}{1-r_N^A(x,\phi) r_N^B(x,\phi) e^{-x}}. \quad (2)$$

The reflection coefficients for the composite slab $A(B)$ $r_N^{A(B)}$ in Eq. (1) are given by

$$r_{\mathrm{TE}}^{A(B)} = \frac{\sqrt{k^2+\xi^2/c^2} - \sqrt{k^2+\varepsilon_e^{A(B)}(i\xi)\xi^2/c^2}}{\sqrt{k^2+\xi^2/c^2} + \sqrt{k^2+\varepsilon_e^{A(B)}(i\xi)\xi^2/c^2}},$$

$$r_{\mathrm{TM}}^{A(B)} = \frac{\varepsilon_e^{A(B)}(i\xi)\sqrt{k^2+\xi^2/c^2} - \sqrt{k^2+\varepsilon_e^{A(B)}(i\xi)\xi^2/c^2}}{\varepsilon_e^{A(B)}(i\xi)\sqrt{k^2+\xi^2/c^2} + \sqrt{k^2+\varepsilon_e^{A(B)}(i\xi)\xi^2/c^2}}. \quad (3)$$

For composite material slab A (or B), the ellipsoidal metal particles are randomly oriented, and each particle is assumed to be described by three depolarization factors L_x, L_y, and L_z, satisfying the sum rule $L_x + L_y + L_z = 1$. For simplicity, we assume all ellipsoids to be ellipsoids of rotation with the symmetry axis along the z axis, $L_x = L_y$. For a given L_z, one yields $L_x = L_y = (1-L_z)/2$. As a consequence, one can use only one depolarization factor L_z to characterize the shape of the ellipsoid. For instance, L_z equals $1/3$ for spherical particles, $0 < L_z < 1/3$ denotes a prolate spheroid, and $1/3 < L_z < 1$ denotes an oblate spheroid. Furthermore, the clustering of spherical particles and their resulted dipole-dipole interaction can be phenomenologically taken into account via a set of effective depolarization factors [32]. These depolarization factors are, generally speaking, fictitious, not real quantities, and hence are not related to real ellipsoidal shape. In particular, it was shown that for double spheres and linear chains, the particle aggregates behave like prolate spheroids, while for three-dimensional fcc lattices they behave like oblate spheroids [33].

Then, we consider the embeddings of both spheroidal metal particles and spherical dielectric particles in a uniform medium to derive the effective permittivity of the composites. Since spheroidal particles are randomly oriented, the average over all orientations of the polarization density produced in metal and dielectric particles, respectively, can be written as [24,28,34]

$$\langle P\rangle_1 = \frac{1}{3}\left[\frac{\varepsilon_1-\varepsilon_e}{\varepsilon_e + L_z(\varepsilon_1-\varepsilon_e)} + \frac{2(\varepsilon_1-\varepsilon_e)}{\frac{(1-L_z)}{2}\varepsilon_1 + \frac{(1+L_z)}{2}\varepsilon_e}\right],$$
$$\langle P\rangle_2 = 3\frac{\varepsilon_2-\varepsilon_e}{\varepsilon_2+2\varepsilon_e}. \quad (4)$$

The effective permittivity $\varepsilon_e^{A(B)}$ can then be established by imposing the consistency requirement that the arithmetic average of the polarization density over metal and dielectric particles vanishes $f\langle P\rangle_1 + (1-f)\langle P\rangle_2 = 0$, that is

$$f(\varepsilon_1-\varepsilon_e)\left[\frac{1}{\varepsilon_e + L_z(\varepsilon_1-\varepsilon_e)} + \frac{4}{(1-L_z)\varepsilon_1 + (1+L_z)\varepsilon_e}\right] + 9(1-f)\frac{\varepsilon_2-\varepsilon_e}{\varepsilon_2+2\varepsilon_e} = 0. \quad (5)$$

Equation (5) can be considered as the generalized Bruggeman effective medium approximation (GEMA).

What is the need to consider such a generalization? In fact, the conventional Bruggeman effective medium approximation (BEMA) is, probably, the most popular phenomenological approximation used to describe the effective conductivity and permittivity of various composite systems. The issues of its applicability and realizability of corresponding microgeometries have been discussed in many papers. Among them, we especially notice the work by Milton [35] who has considered the problem in terms of the coherent potential approximation. In particular, the following points, stemming from Milton's

study, are noteworthy. (i) Milton has shown that the BEMA is exact for a wide class of composites made of spherical particles. To fill all space, the spheres must have a range of sizes (obviously, at least one of composite phases must include zero-radius particles to fill empty cavities between spheres), and to avoid clustering on a macroscopic scale, the spatial distribution of the particles must satisfy a homogeneity condition. (ii) Most of Milton's analysis can be extended to model composites with nonspherical particles. In particular, no obvious obstacles exist to generalize Milton's analysis to particles with smooth surfaces. Therefore, in our situation, in order to fill the whole space, the ellipsoids and/or spheres must have distribution in sizes including infinitesimally small particles, while keep the same shape or aspect ratio. (iii) The treatment of the depolarization factor L_z in Eq. (5) as the effective one allows one to consider this equation as a generalization of the BEMA for spherical particles with allowance for the particle clustering.

In spite of its popularity, the conventional BEMA has the disadvantage. For instance, although it predicts the percolation threshold, its fixed and high value ($f_c = 1/3$) is an exception rather than a rule; in fact, the percolation threshold should depend on actual microgeometry and is usually lower than 1/3 in three-dimensional composites [36]. At the same time, GEMA is free of the above disadvantage. Indeed, the percolation threshold for GEMA is found to be [24,29,34]

$$f_c = \frac{9L_z(1-L_z)}{-9L_z^2+15L_z+2}. \tag{6}$$

As is easy to check from Eq. (6), the percolation threshold peaks at $L_z = 1/3$ (for spheres) and then it monotonically approaches zero as $L_z \to 0$ or $L_z \to 1$.

On the other hand, for the composite slab with asymmetric microstructure, in which randomly oriented, ellipsoidal metal particles with volume fraction f are embedded in a dielectric host medium with volume fraction $1-f$, the effective permittivity can be described by the generalized Maxwell-Garnett approximation [23],

$$\varepsilon_e = \varepsilon_2\left\{1+\frac{f}{3}\left[\frac{\varepsilon_1-\varepsilon_2}{\varepsilon_2+L_z(\varepsilon_1-\varepsilon_2)} + 4\frac{\varepsilon_1-\varepsilon_2}{2\varepsilon_2+(1-L_z)(\varepsilon_1-\varepsilon_2)}\right]\right\}. \tag{7}$$

Note that in comparison with Eq. (5), Eq. (7) is valid for not too large volume fractions and does not predict the percolation transition. For composite slabs A and B with different volume fraction f or different L_z, the effective permittivity for slabs A and B predicted by Eq. (5) and/or Eq. (7) should be quite different. As a consequence, our formulas are applicable for the situation in which two composite slabs are not identical. Substituting Eqs. (5) and/or (7) into Eq. (3), and then Eq. (2), one may estimate the Casimir force between two infinite composite slabs with symmetric or asymmetric microstructures. For simplicity, we assume the two composite slabs have the same microstructures with the same physical and geometric parameters.

III. NUMERICAL RESULTS

We are now in a position to present numerical results for Casimir force between two infinite composite slabs containing nonspherical metal particles. For this purpose, we shall describe the permittivity $\varepsilon(i\xi)$ of the material at the imaginary frequencies from the available data $\varepsilon''(\omega)$ according to the Kramers-Kronig relations

$$\varepsilon(i\xi) = 1+\frac{2}{\pi}\int_0^\infty d\omega\frac{\omega\varepsilon''(\omega)}{\omega^2+\xi^2}. \tag{8}$$

For gold, we have [14]

$$\varepsilon_1(i\xi) = 1+\varepsilon_I(i\xi)+\varepsilon_{II}(i\xi)+\varepsilon_{III}(i\xi), \tag{9}$$

where $\varepsilon_I(i\xi)$ is integrated in the frequency region from zero to the cutoff frequency 0.125 eV from the Drude model of the metal with the form [12,14,22]

$$\varepsilon_I(i\xi) = \frac{2}{\pi}\frac{\omega_{pe}^2}{\xi^2-\omega_c^2}\left[\arctan\left(\frac{\omega_c}{\gamma_e}\right)-\frac{\gamma_e}{\xi}\arctan\left(\frac{\omega_c}{\xi}\right)\right], \tag{10}$$

with the plasma frequency $\omega_{pe} = 9.0$ eV and the damping coefficient $\gamma_e = 0.035$ eV. In addition, $\varepsilon_{II}(i\xi)$ and $\varepsilon_{III}(i\xi)$ can, respectively, be calculated by integrating the polynomial expressions, which are fitted for $\omega_c < \omega < \omega_0$ and $\omega > \omega_0$ ($\omega_0 \sim 2.45$) eV for the tabulated data of Au from Palik [37].

The permittivity of SiO_2 in the imaginary frequency is described by an oscillator model [22,37],

$$\varepsilon_2(i\xi) = 1+\frac{C_{\rm UV}}{1+(\xi/\omega_{\rm UV})^2}+\frac{C_{\rm IR}}{1+(\xi/\omega_{\rm IR})^2}, \tag{11}$$

where $C_{\rm IR}$ ($C_{\rm UV}$) is the absorption strength in the infrared (ultraviolet) region and $\omega_{\rm IR}$ ($\omega_{\rm UV}$) is the corresponding frequency.

In Fig. 1, the effective permittivity ε_e of the composite slab with symmetric microstructure is plotted as the function of the depolarization factor L_z. For small frequency $\xi = 0.02\omega_p$ [see Fig. 1(a)], the permittivity of nonspherical Au particles is much larger than that of SiO_2 particles, and Au metal particles should dominate the behavior of the composites. As a consequence, one observes that the effective permittivity ε_e is strongly dependent on the shape or the depolarization factor of Au particles. In detail, ε_e exhibits nonmontonic behavior with increasing L_z, i.e., first, it decreases, reaches a minimum for spherical shape $L_z = 1/3$, and then it increases. In other words,

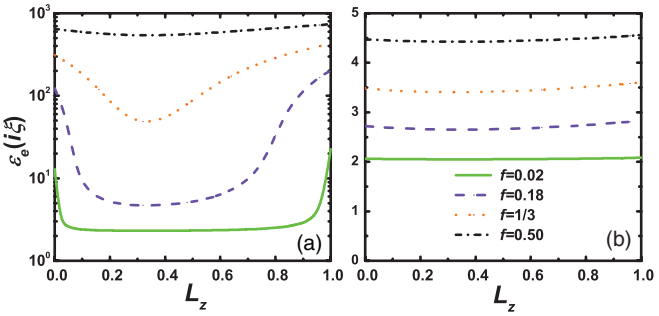

FIG. 1. (Color online) Effective permittivity ε_e of nonspherical composite materials as a function of the shape L_z for (a) $\xi = 0.02\omega_p$ and (b) $\xi = 0.5\omega_p$.

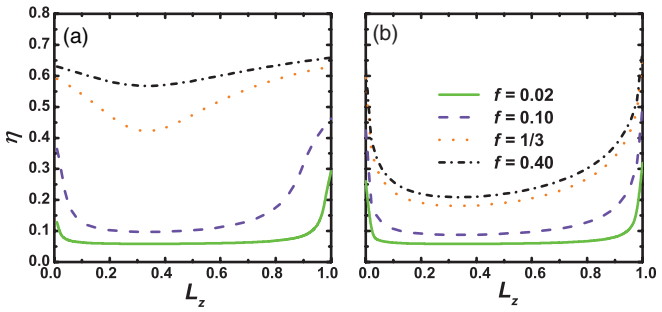

FIG. 2. (Color online) Normalized Casimir force η as a function of L_z in (a) (GEMA) and (b) (GMGA) for various f and $d = 500$ nm.

when the shape of Au particles deviates from the spherical one, the effective permittivity will become large regardless of the prolate ($L_z < 1/3$) or the oblate ($L_z > 1/3$) shape. However, for large frequency $\xi = 0.5\omega_p$ [see Fig. 1(b)], the permittivity of Au can be comparable to the permittivity of SiO_2, resulting in weak dependence of ε_e on the particles' shape L_z. Moreover, it is seen that the effective permittivity ε_e is increased with the increase of the volume fraction f, as expected. Therefore, the shape of Au particles L_z and the volume fraction f may play important roles in determining the magnitude of the Casimir force between two composite slabs.

It is known that the main contributions of the Casimir force come from the frequencies in the vicinity of $\omega \sim c/2d$ (the corresponding wavelengths about the order of $\lambda \sim 4\pi d$), where d is the corresponding separation of two material slabs [12,14,22]. In order to investigate the Casimir force between two composite materials, the separation between two composite materials and the size of granular inclusions a should satisfy the condition $4\pi d \gg a$. If the typical size of the granular inclusions considered in the composite material is about $a = 20$ nm, the corresponding separations of two material slabs should be larger than $d \gg 2$ nm. In Fig. 2, we investigate the effect of L_z on the normalized Casimir force η between two composite slabs with symmetric microstructures [see Fig. 2(a)] and asymmetric ones [see Fig. 2(b)] for large distance $d = 500$ nm. Since the main contribution to the Casimir force comes from the frequencies $\xi < c/d$, the larger d is, the larger the weight of contributions from low frequencies to η is. As a result, one observes the dependence of η on L_z is quite similar as the dependence of ε_e on L_z in the low-frequency case, i.e., η is quite sensitive to L_z [see Fig. 2(a)]. Especially, we find that the normalized Casimir force is smallest for the spherical Au particles ($L_z = 1/3$), and the adjustment of the particles' shape far from the spherical one results in large ε_e and η. This indicates that the spherical particle clustering, which can be described via a change of the depolarization factors, results in an increase of the Casimir force. We further find that η exhibits weak dependence on L_z for large volume fractions such as $f = 0.5$. Actually, in this situation, the nonspherical Au particles can easily form an infinite clusters through the whole composite, and the percolation effect takes place. For small volume fraction such as $f = 0.02$, one observes that η keeps invariant in most region $0 < L_z < 1$ due to the fact that the Casimir force is mainly determined by the spherical SiO_2 particles. However, for needlelike ($L_z \to 0$) and disklike ($L_z \to 1$) shapes, the percolation effect can still occur even for small volume fraction

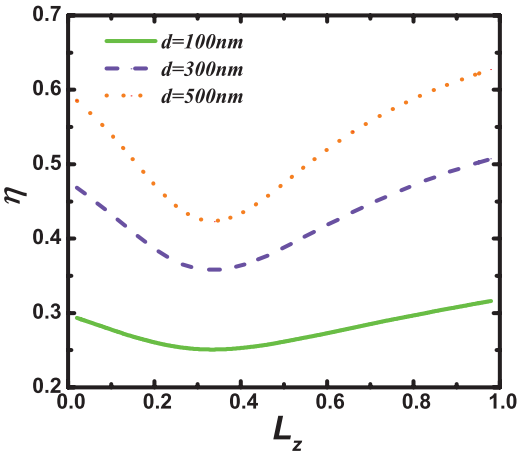

FIG. 3. (Color online) η versus L_z for $f = 1/3$.

of Au, resulting in much larger η in comparison with the force for the system containing both spherical metal and dielectric spherical particles. As for the composite slabs with asymmetric microstructures [see Fig. 2(b)], for small volume fractions such as $f = 0.01$, both the magnitude for η and the dependence of η on L_z based on GMGA [Eq. (7)] are almost the same as those based on GEMA [Eq. (5)]. However, for large volume fractions such as $f = 1/3$ and $f = 0.4$, in general, GMGA gives smaller Casimir force than GEMA does due to the metal-insulator transition predicted by GEMA [22].

Then, the Casimir force based on GEMA as a function of the depolarization factor L_z is plotted in Fig. 3 for different separations d. Again, η exhibits nonmonotonic behavior with increasing L_z and has a minimum for spherical metal particles ($L_z = 1/3$). In addition, the magnitude of the Casimir force becomes large with the increase of the separations. The physical origin can be understood as follows: when the separation is small (large), i.e., c/d is large (small), the weight of the contributions from the high (low) -frequency region in the Casimir force will increase. Correspondingly, the effective permittivity ε_e at the high (low) frequency is small (large), resulting in small (large) Casimir force.

Next, we study the effect of the volume fraction f on the Casimir force based on GEMA for different depolarization factors L_z, as shown in Fig. 4. η increases as the volume

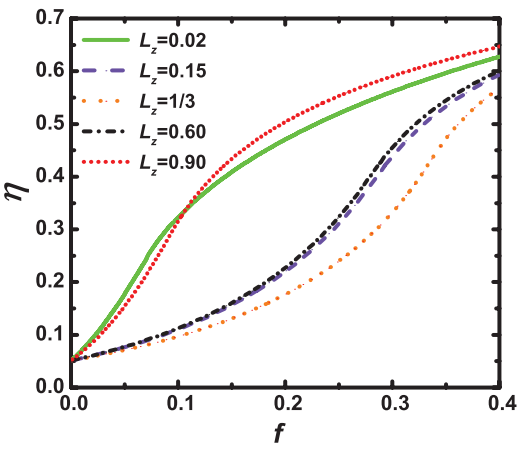

FIG. 4. (Color online) η versus f for $d = 500$ nm.

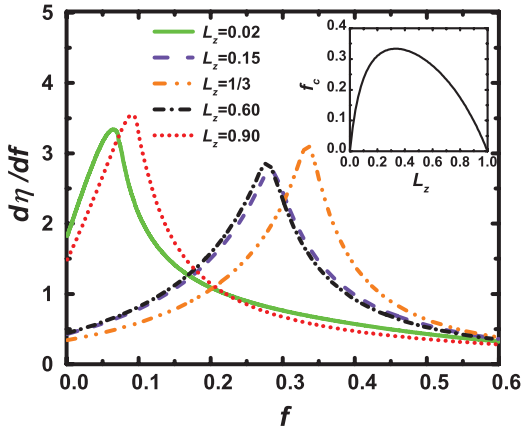

FIG. 5. (Color online) $d\eta/df$ versus f for various L_z and for $d = 500$ nm. Note that, for each curve, there is a maximal value at the corresponding percolation threshold. The percolation threshold as a function of L_z is plotted in the inset.

fraction increases in all cases, which are quite similar as those reported in Ref. [22] for spherical composite materials. Actually, for the composite material with spherical particles ($L_z = 1/3$), the percolation threshold f_c is $1/3$. For $f > f_c$, the composite is metallic, while for $f < f_c$, the composite is pure dielectric. Therefore, metal-insulator transition in composite material can take place, resulting in the drastic change of the Casimir force at the percolation threshold $f_c = 1/3$ (see the case for $L_z = 1/3$). For $L_z \neq 1/3$, the percolation threshold is less than $1/3$, and the drastic increase of η with f occurs at small volume fractions for both prolate ($L_z < 1/3$) and oblate ($L_z > 1/3$) particles. In order to show this, we calculate the slope of the η-f curve, i.e., $d\eta/df$ as a function of f in Fig. 5. It is evident that, for a given L_z, there is a critical volume fraction, at which the slope $d\eta/df$ is maximal. The maximal slope just indicates that the Casimir force exhibits the fastest increase at such a critical volume fraction. Actually, this critical volume fraction is nothing but the percolation threshold for the given L_z (see the inset). Therefore, one should observe the fastest change of the Casimir force at the percolation threshold f_c, at which the metal-insulator phase transition occurs for the composite slabs with symmetric microstructures. Incidentally, for the composite slabs with asymmetric microstructures, $d\eta/df$ is expected to exhibit monotonic behavior with f, indicating no percolation effect with GMGA.

IV. CONCLUSIONS

The Casimir force between two semi-infinite slabs made of the metal-dielectric composite material is investigated by Casimir-Lifshitz theory. The composite material slab may have the symmetric microstructure, in which randomly oriented nonspherical metal particles and spherical dielectric particles are randomly mixed and the effective permittivity is predicted by GEMA, or the asymmetric microstructure, in which randomly oriented nonspherical metal particles are embedded in the dielectric host and the effective permittivity is predicted by GMGA. Numerical results show that the Casimir force is strongly dependent on the particles' shape. When metal particles are spherical in shape ($L_z = 1/3$), the magnitude of the Casimir force is minimal, and the adjustment of the particles' shape far from spherical shape results in the enhancement of the Casimir force. In addition, within GEMA, the curve for the Casimir force η against the volume fraction f exhibits a fast increase with the increase of f at the percolation threshold f_c, which is determined by the particles' shape. Therefore, the particles' shape plays a crucial role in determining the magnitude of the Casimir force between two inhomogeneous composite slabs containing nonspherical metal particles.

Some comments are in order. Our theoretical predictions of the Casimir force, including its nonmonotonic dependence on the particles' shape and metal-insulator transition, have yet to be observed experimentally. Fortunately, some techniques have been developed to fabricate nonspherical metal particles by lithographic means [38] and even to realize the morphology control with colloid-chemical synthesis [39]. In addition, the composite media containing nonspherical metal particles were fabricated and characterized [40]. With the development of the Casimir measurements and the metal-dielectric composites manufactured in recent years, it is expected that the Casimir measurement of ellipsoidal shape effects in composite materials will be feasible in the near future, and an interesting question whether the Casimir force can undergo a fast change near the metal-insulator phase transition can be checked. In addition, we adopt GEMA and GMGA to predict the effective permittivity of the inhomogeneous metal-dielectric composite materials containing nonspherical particles. Generally, the sizes of metal-dielectric particles are about 10 nm, and the nonlocality or spatial dispersion should be taken into account. In this connection, the nonlocal effective-medium theory can be adopted, in order to make the precise calculation of the Casimir force between the composite materials. Work along this line is in progress and we shall report it elsewhere.

ACKNOWLEDGMENTS

The authors thank Professor P. M. Hui and Professor D. J. Bergman for valuable discussions. This work was supported by the National Natural Science Foundation of China under Grant No. 11074183, the National Basic Research Program under Grant No. 2012CB921501, the Key Project in Natural Science Foundation of Jiangsu Education Committee of China under the Grant No. 10KJA140044, the Key Project in Science and Technology Innovation Cultivation Program, the Plan of Dongwu Scholar, Soochow University, and the Project Funded by the Priority Academic Program Development of Jiangsu Higher Education Institutions.

[1] H. B. G. Casimir, Proc. K. Ned. Akad. Wet. **51**, 793 (1948).
[2] S. K. Lamoreaux, Phys. Rev. Lett. **78**, 5 (1997).
[3] U. Mohideen and A. Roy, Phys. Rev. Lett. **81**, 4549 (1998).
[4] M. Boström and B. E. Sernelius, Phys. Rev. Lett. **84**, 4757 (2000).
[5] G. Bressi, G. Carugno, R. Onofrio, and G. Ruoso, Phys. Rev. Lett. **88**, 041804 (2002).

[6] R. S. Decca, D. López, E. Fischbach, and D. E. Krause, Phys. Rev. Lett. **91**, 050402 (2003).
[7] J. N. Munday, F. Capasso, and V. A. Parsegian, Nature (London) **457**, 170 (2009).
[8] A. Lambrecht, P. A. Maia Neto, and S. Reynaud, New J. Phys. **8**, 243 (2006).
[9] M. Bordag, G. L. Klimchitskaya, U. Mohideen, and V. M. Mostepanenko, *Advances in the Casimir Effect* (Oxford University Press, Oxford, 2009).
[10] *Casimir Physics*, edited by D. Dalvit, P. Milonni, D. Roberts, and F. Rosa, Lecture Notes in Physics (Springer, Berlin, Heidelberg, 2011).
[11] A. W. Rodriguez, F. Capasso, and S. G. Johnson, Nat. Photon. **5**, 211 (2011).
[12] I. Pirozhenko, A. Lambrecht, and V. B. Svetovoy, New J. Phys. **8**, 238 (2006).
[13] A. Lambrecht, I. Pirozhenko, L. Duraffourg, and Ph. Andreucci, Europhys. Lett. **77**, 44006 (2007).
[14] V. B. Svetovoy, P. J. van Zwol, G. Palasantzas, and J. Th. M. De Hosson, Phys. Rev. B **77**, 035439 (2008).
[15] R. Esquivel-Sirvent, M. Palomino-Ovando, and G. H. Cocoletzi, Appl. Phys. Lett. **95**, 051909 (2009).
[16] V. A. Yampol'skii, S. Savel'ev, Z. A. Mayselis, S. S. Apostolov, and F. Nori, Phys. Rev. Lett. **101**, 096803 (2008).
[17] Y. P. Yang, R. Zeng, J. P. Xu, and S. T. Liu, Phys. Rev. A **77**, 015803 (2008).
[18] F. S. S. Rosa, D. A. R. Dalvit, and P. W. Milonni, Phys. Rev. Lett. **100**, 183602 (2008).
[19] R. Zhao, J. Zhou, Th. Koschny, E. N. Economou, and C. M. Soukoulis, Phys. Rev. Lett. **103**, 103602 (2009).
[20] R. Esquivel-Sirvent, J. Appl. Phys. **102**, 034307 (2007).
[21] M. G. Silveirinha and S. I. Maslovski, Phys. Rev. A **82**, 052508 (2010).
[22] R. Esquivel-Sirvent and G. C. Schatz, Phys. Rev. A **83**, 042512 (2011).
[23] L. Gao, K. W. Yu, Z. Y. Li, and B. Hu, Phys. Rev. E **64**, 036615 (2001).
[24] L. H. Shi, L. Gao, S. L. He, and B. W. Li, Phys. Rev. B **76**, 045116 (2007).
[25] L. H. Shi and L. Gao, Phys. Rev. B **77**, 195121 (2008).
[26] D. L. Gao and L. Gao, Appl. Phys. Lett. **97**, 041903 (2010).
[27] F. Brouers, J. Phys. C: Solid State Phys. **19**, 7183 (1986).
[28] T. W. Noh, P. H. Song, and A. J. Sievers, Phys. Rev. B **44**, 5459 (1991).
[29] L. Gao and Z. Y. Li, J. Phys.: Condens. Matter **15**, 4397 (2003).
[30] E. G. Galkina, B. A. Ivanov, S. Savel'ev, V. A. Yampolskii, and F. Nori, Phys. Rev. B **80**, 125119 (2009).
[31] C. Raabe, L. Knöll, and D. G. Welsch, Phys. Rev. A **68**, 033810 (2003).
[32] P. Clippe, R. Evrard, and A. A. Lucas, Phys. Rev. B **14**, 1715 (1976).
[33] C. G. Granqvist and O. Hunderi, Phys. Rev. B **16**, 3513 (1977).
[34] L. Gao and Y. Ma, J. Phys. A: Math. Gen. **38**, 7765 (2005).
[35] G. W. Milton, Commun. Math. Phys. **99**, 463 (1985).
[36] A. V. Goncharenko, Phys. Rev. E **68**, 041108 (2003).
[37] *Handbook of Optical Constants of Solids*, edited by E. D. Palik (Academic Press, Orlando, 1995).
[38] B. M. I. V. D. Zande, L. Pages, R. A. M. Hikmet, and A. V. Blaaderen, J. Phys. Chem. B **103**, 5761 (1999).
[39] T. K. Sau and A. L. Rogach, Adv. Mater. **22**, 1781 (2010).
[40] H. B. Liao, W. Wen, and G. K. L. Wong, Appl. Phys. A **80**, 861 (2005).